Supporting Information

Electrochemical Strain Dynamics in Noble Metal Nanocatalysts

Raphaël Chattot [1,], Isaac Martens [1], Marta Mirolo [1], Michal Ronovsky [1], Florian Russello [1], Helena Isern Herrera [1], Guillaume Braesch [2], Elisabeth Hornberger [3], Peter Strasser [3], Eric Sibert [2], Marian Chatenet [2], Veijo Honkimäki [1], and Jakub Drnec [1]*

[1] European Synchrotron Radiation Facility, ID 31 Beamline, BP 220, F-38043 Grenoble, France

[2] Univ. Grenoble Alpes, Univ. Savoie Mont Blanc, CNRS, Grenoble INP*, LEPMI, 38000 Grenoble, France. *Institute of Engineering and Management Univ. Grenoble Alpes

[3] Electrochemical Energy, Catalysis and Material Science Laboratory, Department of Chemistry, Technische Universität Berlin, 10623 Berlin, Germany

*e-mail: (RC) raphael.chattot@grenoble-inp.org

This File includes:

Experimental Methods

Electrocatalysts

For the Palladium experiment, a Pd/Vulcan XC72® catalyst with a Pd weight fraction (wt.%) of 20% was purchased from Premetek and used as reference material without any treatment. For the Platinum experiment in alkaline electrolyte, a Pt/Vulcan XC72® catalyst with a Pt weight fraction (wt.%) of 20% (TEC10V20E) was purchased from Tanaka Kikinzoku Kogyo (TKK) and used as reference material without any treatment. For the Platinum experiment in acidic electrolyte, a Pt/Vulcan XC72® catalyst with a Pt weight fraction (wt.%) of 25% was prepared via wet impregnation followed by thermal reduction in hydrogen atmosphere in a fluidized bed reactor as reported elsewhere [1]. A mixture of hexachloroplatinic acid (IV) hexahydrate (99.95% metal basis, Pt 37.5% min, Alfa Aesar) and carbon support material (Vulcan XC72R®, Cabot Corporation) in a 1:2 solution of ultrapure water (Milli-Q, 18.2 MΩ·cm) and isopropanol (AnalaR NORMAPUR, VWR) was homogenized for 15 min using a horn sonifier. The formed slurry was quenched in liquid nitrogen and dried in vacuum. The dry sample was placed in a fluidized bed reactor and after purging the reactor with nitrogen, the atmosphere was switched to 4% H_2 in Ar. The temperature was raised with a heating rate of 5 K min^{-1} to 200 °C and held for 2 h. After that, the sample was cooled down to room temperature in nitrogen atmosphere within 15 min.

Electrochemical Measurements

All the glassware accessories and cell components used in this study were firstly cleaned by soaking in a H_2SO_4:H_2O_2 mixture for at least 12 hours and thoroughly washed in Milli-Q water (Millipore, 18.2 MΩ cm, total organic compounds < 3 ppb). A Biologic potentiostat SP300 and custom-made three-electrode electrochemical flow cells were used. The electrolyte (0.1 M NaOH, Suprapur®, Merck or 0.1 M $HClO_4$, Suprapur®, Merck) was prepared prior each sample measurement and flowed constantly through the cell at a rate of 20 mL min^{-1} using a peristaltic pump. The counter-electrode

was a Pt wire and the reference electrode a commercial Hg/HgO electrode (OrygaLys) in case of Pd, and a commercial leakless miniature Ag/AgCl electrode (ET072, eDAQ) in case of Pt.

To prepare the thin-film working electrodes for transmission geometry, 20 µL of a catalytic ink suspension containing 2.3 g_{metal} L^{-1} was pipetted and dried on a 16 mm diameter disk commercial gas diffusion electrode (Freundenberg, WE-95-2SH). The diameter of the as-formed catalytic film was typically around 2 mm, corresponding to a metal loading of 1.45 mg_{metal} cm^{-2}. The ink suspensions were composed of 29 mg of catalyst powder (20 wt.% metal), 154 µL of 5 wt.% Nafion® solution (Electrochem. Inc.), 743 µL of isopropanol and 1.8 mL (18.2 MΩ cm) of deionized water (MQ-grade, Millipore). For the grazing incidence geometry, 10 µL of a catalytic ink suspension containing 0.49 g_{metal} L^{-1} was pipetted and dried on a 5 mm diameter mirror-polished glassy carbon cylinder, thus reaching a metal loading of 25 μg_{metal} cm^{-2}. The ink suspensions were composed of 10 mg of catalyst powder (25 wt.% metal), 54 µL of 5 wt. % Nafion® solution (Electrochem. Inc.), 1446 µL of isopropanol and 3.6 mL (18.2 MΩ cm) of deionized water (MQ-grade, Millipore).

Synchrotron Wide-Angle X-Ray Scattering (WAXS) Measurements

Synchrotron WAXS measurements were performed at ID31 beamline of the European Synchrotron Radiation facility (ESRF) in Grenoble, France. The high energy X-ray beam (78 keV) was focused on the catalyst powders through the cells in transmission or grazing incidence modes, and the scattered signal was collected using a Dectris Pilatus CdTe 2M detector positioned 850 mm behind the sample. The energy, detector distance and tilts were calibrated using a standard CeO_2 powder and the 2D diffraction patterns were reduced to the presented 1D curves using the pyFAI software package [2].

Rietveld Refinements

Rietveld refinement of the WAXS patterns was performed to extract the phase structure, crystallite size, lattice parameter and microstrain using the *Fm3m* structure of Pd and Pt metal and the Fullprof

software. The instrumental resolution function was determined by the refinement of a CeO_2 standard sample. Thomson-Cox-Hastings profile function was adopted [3]. The background of patterns was described by an interpolated set of points with refinable intensities.

Method to correct the microstructural data from nanoparticle size

Since the size of a nanoparticle controls its surface-to-volume ratio, structural changes occurring on a nanoparticle surface, when measured with a bulk technique, are expected to be more or less masked/compensated by the structure of the core. Consequently, when comparing the effects of electrochemical adsorbates formation on lattice constants and/or scale factors changes for materials featuring different nanoparticle sizes, a correction from this phenomenon is desirable.

The dispersion (*D*, in %), or the proportion of atoms being located at the surface of a nanoparticle can be calculated from Montejano-Carrizales *et al.* model of face-centred cubic cuboctahedral particles [4,5]:

$$D = 100\frac{Ns}{N} \qquad \text{Eq. S1}$$

Where *N* and *N*s are the total number of atoms and the number of surface atoms, respectively:

$$N = 10\frac{m^3}{3} + 5m^2 + \frac{11}{3}m + 1 \qquad \text{Eq. S2}$$

$$Ns = 10m^2 + 2 \qquad \text{Eq. S3}$$

'm' corresponds to the number of atomic layers composing the crystallite in the Montejano-Carrizales model. The values of '*m*' are linked to the crystallite size '*d'* by the relation:

$$m = \frac{d}{2\sqrt{3}r_{\text{atom}}} \qquad \text{Eq. S4}$$

With 'r_{atom}' being the covalent radius of the atom (r_{Pt} = 0.135 nm and r_{Pd} = 0.140 nm).

In this study, the dispersion *D* is calculated for each catalyst based on its measured crystallite size *d* from WAXS. The values of *D* were found to be 37.3 % and 23.6 % for Pt and Pd, respectively.

The size-corrected relative variations (in %) of a parameter *x* is thus defined as

$$f(x) = \frac{100}{D} * 100 * \frac{x - x_0}{x_0} \qquad \text{Eq. S5}$$

Where x_0 is the reference value of the parameter *x* (here measured at *E* = 0.50 V *vs*. RHE)

Figure S6 shows the evolutions of the lattice constants and scale factors measured during cyclic voltammetry experiment, with different degrees of correction. **Figure S6.a-b** displays the raw parameters without any correction. Because the two materials feature (i) different lattice constants, (ii) nanoparticle sizes and (iii) the quantity of metal under the X-ray beam may differ, the trends are hardly quantitatively comparable. In **Figure S6.c-d**, the relative variation of these parameters compared to their reference values are plotted. These data show that Pt oxidises as much as Pd in these experimental conditions, which is not consistent with the known affinity of these two metals with oxygenated species, and is likely an artefact from the different nanoparticle sizes that are compared. In fact, from the experience of the authors, large nanoparticles (>10 nm) do not even show any measurable lattices or scale factors change due to the fact that the dispersion drops below 13 %. **Figure S6.e-f**, shows the size-corrected relative changes estimated from **Eq. S5**. These are the data are discussed in the main text.

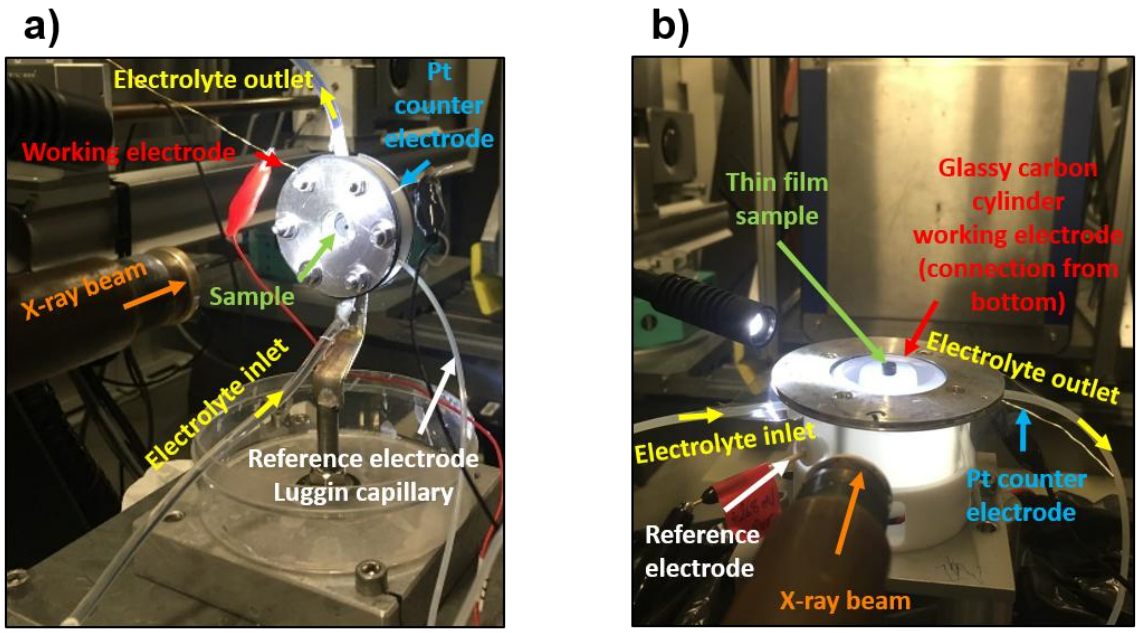

***Supporting Figure S1**: Electrochemical cells for WAXS measurements in (a) transmission configuration and (b) grazing incidence configuration.*

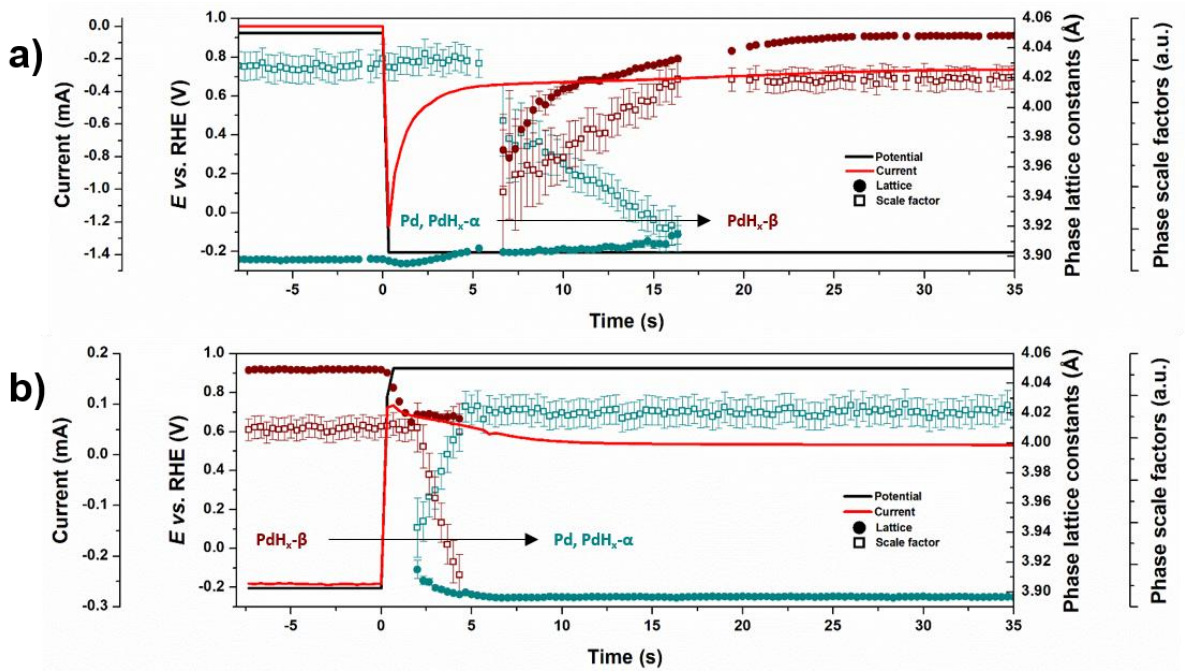

***Supporting Figure S2**: Lattice constants and scale factors evolution recorded during the (a) PdH_x $\alpha \rightarrow \beta$ phase transition triggered by potential step from 0.92V vs. RHE to -0.20 V vs. RH and (b) during the PdH_x $\beta \rightarrow \alpha$ phase transition triggered by potential step from -0.20 V vs. RHE to 0.92 V vs. RHE.*

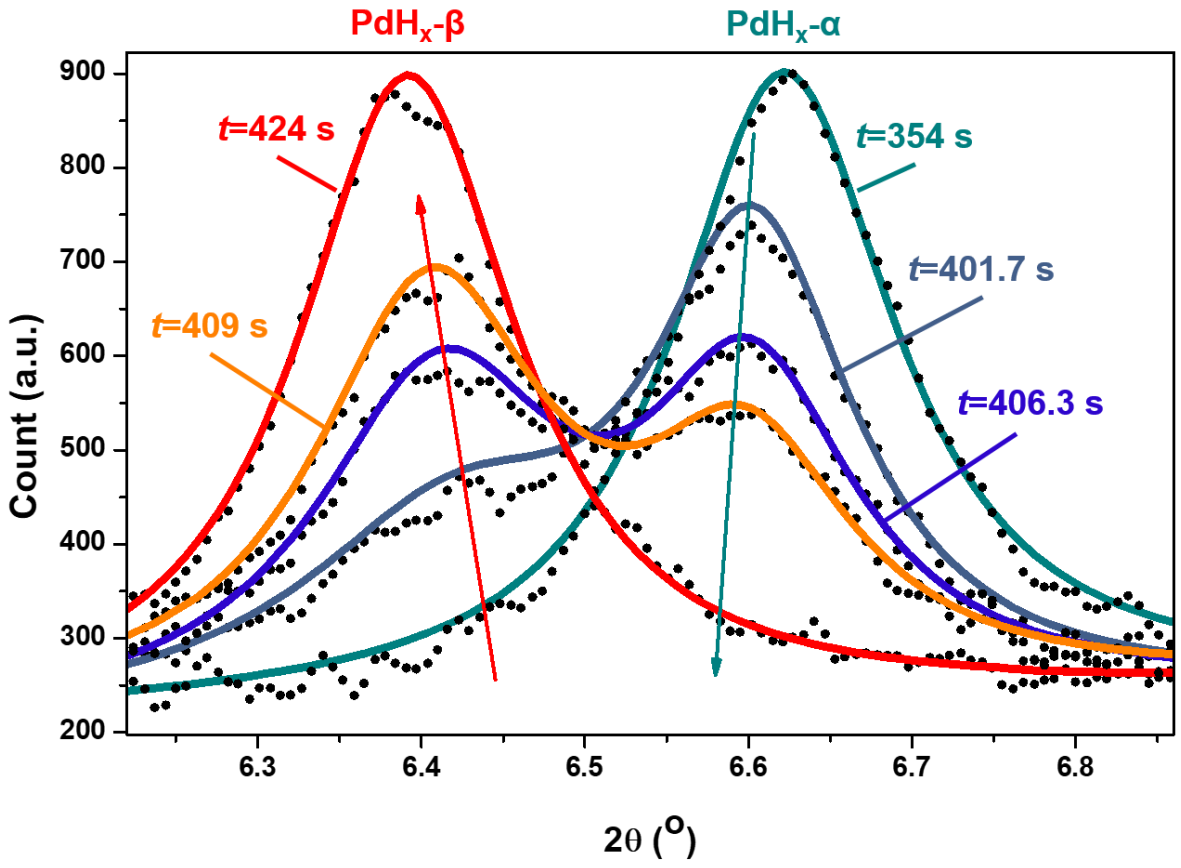

Supporting Figure S3: *Samples of WAXS data and associated Rietveld fits on the Pd [220] Bragg peak reflexion during phase transition showing the angular shifts for the two phases during the transition.*

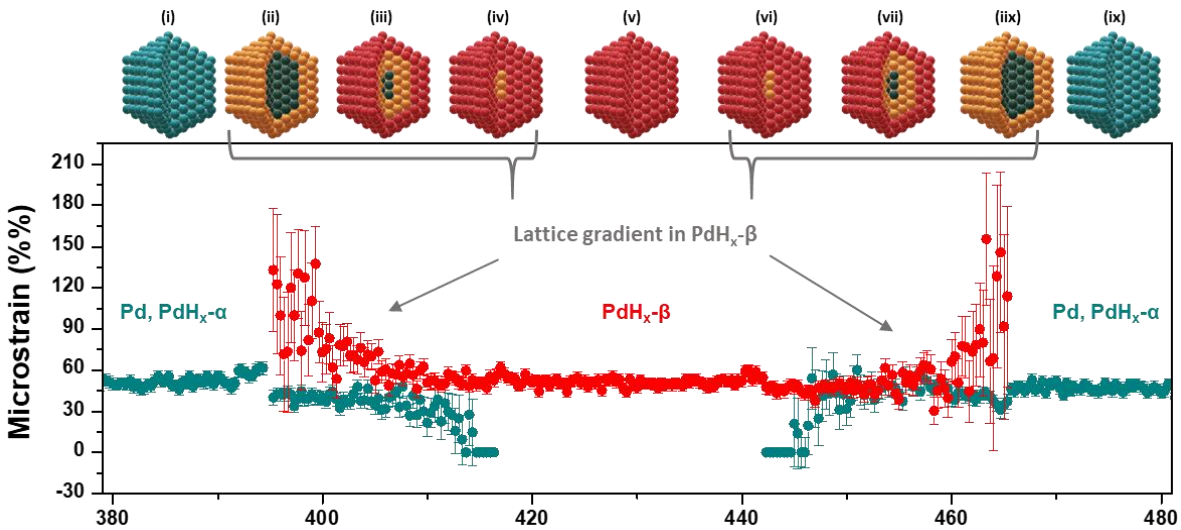

Supporting Figure S4*: Evolution of microstrain values as a function of time for the two PdH_x phases transitions during cyclic voltammetry. Increase in microstrain values indicate increase in lattice constant heterogeneities within the phase.*

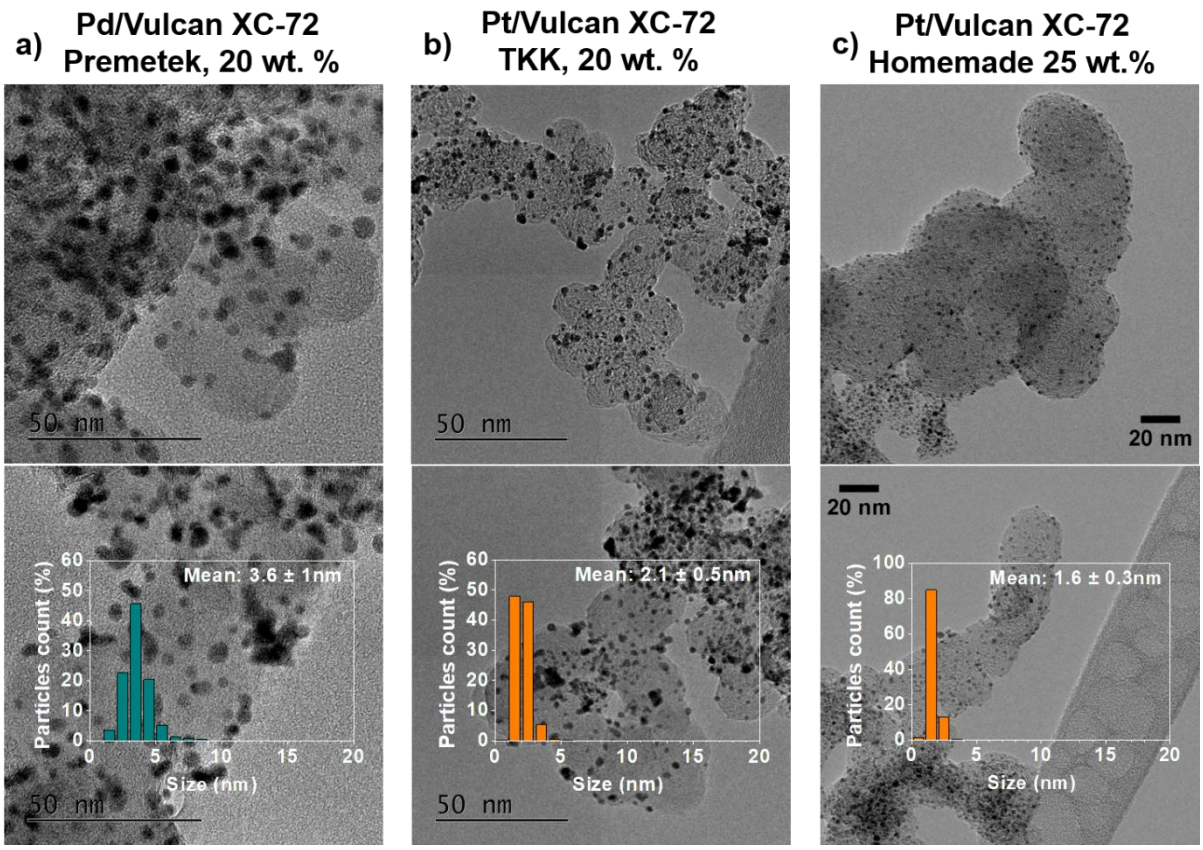

Supporting Figure S5: *Transmission electron microscopy images and corresponding particle size distribution for a) the Pd electrocatalyst from Premetek; b) the Pt electrocatalyst from TKK and c) the homemade Pt/C electrocatalyst used in this study.. a) and b) were studied in alkaline and c) in acid.*

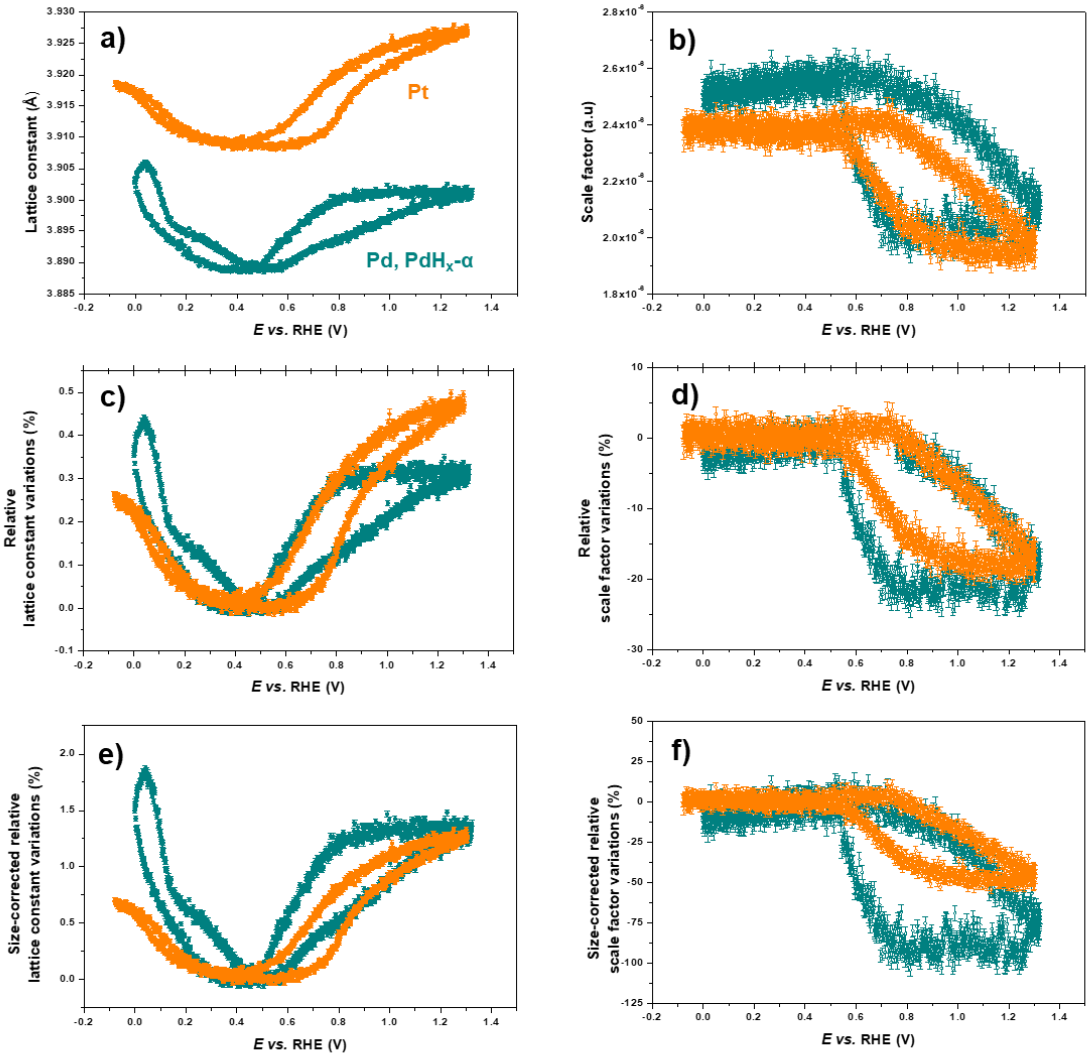

Supporting Figure S6: *Evolutions of the (a-b) raw, (c-d) relative and (e-f) size-corrected relative lattice constants and scale factors variations for Pt (orange) and Pd (cyan) catalysts during cyclic voltammetry in 0.1 M NaOH in room temperature.*

References

1. Hornberger, E., Schmies, H., Paul, B., Kühl, S. & Strasser, P. Design and Validation of a Fluidized Bed Catalyst Reduction Reactor for the Synthesis of Well-Dispersed Nanoparticle Ensembles. *J. Electrochem. Soc.* **167**, 114509 (2020).

2. Ashiotis, G. *et al.* The fast azimuthal integration Python library: PyFAI. *J. Appl. Crystallogr.* **48**, 510–519 (2015).

3. Thompson, P., Cox, D. E. & Hastings, J. B. Rietveld Refinement of Debye-Scherrer Synchrotron X-ray Data from A1203. *J. Appl. Crystallogr.* **20**, 79–83 (1987).

4. Montejano-Carrizales, J. M. & Morán-López, J. L. Geometrical characteristics of compact nanoclusters. *Nanostructured Mater.* **1**, 397–409 (1992).

5. Montejano-Carrizales, J. M., Aguilera-Granja, F. & Morán-López, J. L. Direct Enumeration of the Geometrical Characteristics of Clusters. *Nanostructured Mater.* **8**, 269–287 (1997).